Influence of Alkali Fiber Treatment and Fiber Processing on the Mechanical Properties of Hemp/Epoxy Composites

Mohammad S. Islam,[1*] Kim L. Pickering,[1] Nic J. Foreman[2]

[1]*Department of Engineering, The University of Waikato, Hamilton, New Zealand*
[2]*Hemptech, Herne Bay, Auckland, New Zealand*

Received 3 June 2009; accepted 21 August 2009
DOI 10.1002/app.31335
Published online 6 October 2010 in Wiley Online Library (wileyonlinelibrary.com).

ABSTRACT: Industrial hemp fibers were treated with a 5 wt % NaOH, 2 wt % Na_2SO_3 solution at 120°C for 60 min to remove noncellulosic fiber components. Analysis of fibers by lignin analysis, scanning electron microscopy (SEM), zeta potential, Fourier transform infrared (FTIR) spectroscopy, wide angle X-ray diffraction (WAXRD) and differential thermal/thermogravimetric analysis (DTA/TGA), supported that alkali treatment had (i) removed lignin, (ii) separated fibers from their fiber bundles, (iii) exposed cellulose hydroxyl groups, (iv) made the fiber surface cleaner, and (v) enhanced thermal stability of the fibers by increasing cellulose crystallinity through better packing of cellulose chains. Untreated and alkali treated short (random and aligned) and long (aligned) hemp fiber/epoxy composites were produced with fiber contents between 40 and 65 wt %. Although alkali treatment generally improved composite strength, better strength at high fiber contents for long fiber composites was achieved with untreated fiber, which appeared to be due to less fiber/fiber contact between alkali treated fibers. Composites with 65 wt % untreated, long aligned fiber were the strongest with a tensile strength (TS) of 165 MPa, Young's modulus (YM) of 17 GPa, flexural strength of 180 MPa, flexural modulus of 9 GPa, impact energy (IE) of 14.5 kJ/m^2, and fracture toughness (K_{Ic}) of 5 MPa m$^{1/2}$. © 2010 Wiley Periodicals, Inc. J Appl Polym Sci 119: 3696–3707, 2011

Key words: hemp fiber; thermogravimetric analysis; epoxy resin; mechanical properties; activation energy

INTRODUCTION

The use of plant based fibers as polymer reinforcement has increased over the last few years due to their low cost, low density and good mechanical properties, as well as potential sustainability and biodegradability.[1] The composites produced compare well environmentally with glass fiber reinforced plastics in terms of recyclability when using a thermoplastic matrix and energy recovery through incineration when using a thermoset matrix, as well as generally with traditional structural materials, in terms of their specific mechanical properties.[2] Thermoset polymers are particularly attractive as matrix materials for natural fiber reinforced composite production as they generally have reactive functional groups that make them compatible with hydrophilic fiber surfaces,[2] with epoxies having a major advantage in that they are usually cured in two or more stages which allows preforms to be preimpregnated with the epoxy in a partially cured state.[3]

Industrial hemp is one of the strongest and stiffest available natural fibers.[4] The major constituent of hemp fiber is crystalline cellulose, which can make up 55–72% of the fiber mass.[5] Hemp fiber also contains hemicellulose (8–19%), lignin (2–5%) and smaller amount of waxy substances.[5] However, it is known that lignin and hemicellulose are sensitive to ultra violet (UV) radiation and moisture[6] suggesting that it may be sensible to remove them. However, lignin forms a three dimensional network structure in natural fiber cell walls which suggests complete removal of lignin from fiber would reduce structural integrity.[7]

Alkali treatment with NaOH[8–10] is commonly used to remove noncellulosics from natural fibers. It has also been shown to expose hydroxyl groups and roughen fiber surfaces leading to improved interfacial bonding[11–13] and composite mechanical properties.[13,14] Anhydride modification,[15] organosilane treatment[16] and various coupling agents[17,18] have also been used to improve interfacial bonding, although alkali treatment has been found to be the most feasible.[19] Alkali treatment of fibers has also been seen to increase the crystallinity[6] of cellulose which can lead to an increase in fiber strength; Gassan and Bledzki have obtained an increase in yarn TS and YM of about 120% and 150%, respectively for tossa jute fiber using a 25 wt % NaOH solution.[8]

**Present address:* CSIRO Materials Science and Engineering—Geelong, Belmont 3216, Victoria, Australia.
Correspondence to: M. S. Islam (Saiful.Islam@csiro.au).

In the pulp and paper industry, sodium sulphite (Na_2SO_3) is also commonly used with NaOH during the production of pulp to soften the lignin.[20] Relatively low concentrations of 1.9 wt % NaOH solution containing 0.2 wt % Na_2SO_3 and 0.2 wt % sodium carbonate (Na_2CO_3) have been shown to remove noncellulosic materials from hemp fibers.[21] Geroge et al. have treated nonwoven mats of flax fibers with a mild alkali (1 wt % NaOH) for 1 hr and have reported an improvement of about 13% in TS and 17% in YM for flax/epoxy composites.[22] Mohanty et al. have treated jute fabrics with 5 wt % NaOH at 30°C for 30 min and have reported an improvement of about 43% in TS for jute fabric/polyester amide composites.[23]

Fiber length and orientation of the reinforcing fibers are also important in influencing composite mechanical properties. Composites with longer or more oriented fibers generally exhibit better mechanical properties. A high degree of orientation of long natural fibers can be achieved by creating yarns through textile processing. However, yarns need to have a sufficient level of twist to maintain integrity and the extent of permeability of resins into the yarns decreases with the increase of degree of twist, resulting in low composite strength.[24] Moreover, yarn production requires considerable infrastructure and cost. Alternatively, carding could be used to obtain good orientation in fibers with good fiber separation and almost no twist enabling the resin to permeate into the fibers with ease resulting in good mechanical properties of the composites.

The objective of the current study was to explore the effect of alkalisation with Na_2SO_3 on industrial hemp fiber (by analyzing its lignin and cellulose content, morphology, surface charge, available functional groups, crystallinity index, thermal stability, and tensile properties), fiber length and orientation obtained by carding and dynamic sheet forming on composite mechanical properties.

EXPERIMENTAL

Materials

Retted bast hemp fiber was supplied by Hemcore, UK. Epoxy resin (R180) with an amine curing agent (H180) was obtained from Fiberglass International, Australia. Analytical grade Na_2SO_3 and 98% NaOH pellets were used for the treatment of the fibers.

Treatment of the fibers with alkali

Unwanted pieces of woody core were manually removed from the retted bast hemp fiber. After weighing, fibers were placed into stainless steel canisters of 1 L capacity. Preweighed NaOH and Na_2SO_3 solution was then poured into the canisters such that the fiber to 2 wt % Na_2SO_3 and 5 wt % NaOH solution ratio was 1 : 2 : 10 by weight. The canisters were then placed into a small lab-scale pulp digester at 120°C for 60 min. Fibers were then washed in a pulp and paper fiber washer for about 45 min to remove chemical residues until a fiber pH of about seven was obtained. Fibers were then dried in an oven for 48 h at 70°C.

Lignin and cellulose analysis of the fibers

Lignin and Cellulose analysis was carried out at the Environmental Chemistry Laboratory at Landcare Research New Zealand Limited, in accordance with the terms of International Accreditation New Zealand. The TAPPI Standard Method T 222 (UM 250) was used to determine acid-soluble lignin content. About 0.25 g of sample was ground into fine powder, and the cell wall material was isolated by extraction with a series of solutions and solvents before being analyzed for lignin content. An extinction coefficient (absorptivity) of 110 L/g cm and a filtrate dilution of 1 : 5 were used in these experiments.

Scanning electron microscopy (SEM)

The morphology of the untreated and alkali treated fibers, as well as composite fracture surfaces, were studied using a Hitachi S-4000 Field Emission SEM operated at 5 kV. Carbon tape was used to mount the samples on aluminum stubs. The samples were then sputter coated with platinum and palladium to make them conductive before SEM observation.

Measurement of zeta potential

The zeta potential of untreated and alkali treated fibers was determined in a $1.00 \times 10^{-3}M$ potassium chloride (KCl) electrolyte solution at room temperature using a Mütek SZP 06 System based on the streaming potential method. The pH of the electrolyte solution was varied from 11 to 3. A pH of 11 was obtained using $0.1M$ potassium hydroxide (KOH) solution which was decreased incrementally using $0.1M$ hydrochloric acid (HCl) solution.

Fourier transform infrared (FTIR) spectroscopy

Infrared spectra were obtained using an FTIR Digilab FTS-40 spectrometer. Untreated and alkali treated fibers were ground into small particles in liquid nitrogen and mixed and compressed with potassium bromide (KBr) into a thin disc using a hydraulic press at 8 MPa pressure.

Wide angle X-ray diffraction (WAXRD)

Fiber (0.5 g) was compressed into a tablet using a hydraulic press at 20 MPa pressure. A Philips X-ray diffractometer, employing CuKα (λ = 1.54) radiation and a graphite monochromator with a current of 40 mA and a voltage of 40 mV was used with a diffraction intensity in the range of 6 to 60° (2θ-angle range). The percentage crystallinity index (*CrI*) was determined using the Segal empirical method[25] according to the following equation:

$$\mathrm{CrI} = \frac{I_{002} - I_{\mathrm{am}}}{I_{002}} \times 100 \quad (1)$$

where I_{002} is the maximum intensity of the 002 lattice reflection of the cellulose crystallographic form at $2\theta = 22.5°$ and I_{am} is the intensity of diffraction of the amorphous material at $2\theta = 18.5°$.

Thermal analysis

DTA and TGA were carried out using an SDT 2960 Simultaneous DTA-TGA analyzer. All the measurements were taken whilst maintaining a static air flow of 150 mL/min with a constant heating rate of 10°C/min in an open alumina crucible. The weight of the specimens was around 10 mg, with a scanned temperature range of 25 to 600°C.

Single fiber tensile testing

Single hemp fibers were tensile tested according to the American Society for Testing and Materials (ASTM) D3379-75 standard test method for TS and YM for high-modulus single filament materials. Fibers were separated by hand and attached to cardboard mounting-cards with 10 mm holes punched into them to give a gauge length of 10 mm. Polyvinyl acetate (PVA) glue was used to hold the fibers in place. The fibers were then placed under an optical microscope and inspected with a calibrated eyepiece at 200× magnification to determine the average diameter of each fiber. The mounted fibers were then placed in the grips of an Instron-4204 tensile testing machine, and a hot-wire cutter was used to cut the supporting sides of the mounting cards. Tensile testing of the fibers was carried out to failure at a rate of 0.5 mm/min using a 10 N-load cell. Average TS and YM were obtained using the results from 125 specimens.

Production of preform fiber mats

Short fiber mats

For the production of fiber/epoxy composites, untreated and alkali treated short fibers were initially dried at 80°C for 24 h. Short fiber mats with approximately random orientation were produced by placing 60 g dried short fibers in a compression mould, pouring water over the fibers and then pressing at room temperature. Mats of uniform thickness of 3.5 mm were produced by this technique.

Figure 1 Aligned alkali treated fiber mat produced by dynamic sheet forming (DSF). [Color figure can be viewed in the online issue, which is available at wileyonlinelibrary.com.]

More aligned short fiber mats were produced using dynamic sheet forming. For this, 200 g of fiber was pelletised to lengths of less than 8 mm and then separated with water at 72,000 rpm using a disintegrator. The disintegrated fibers were then used to produce mats of 3 mm thickness using a Centre Technique De L'Industrie Des Papiers Cartons Et Cellulose Dynamic Vertical Former from Ateliers De Construction Allimand, France, which is commonly used for laboratory production of paper. The fiber mats obtained (Fig. 1) were placed in a dryer at 100°C for 24 h and then cut to a size (22 cm long and 15 cm wide) to fit in a compression mould.

Long fiber mats

Aligned long fiber mats were produced by aligning 60 g of fibers using a hand carding machine from Ashford Handicrafts Limited, Ashburton, New Zealand to obtain a thickness of 3.5 mm.

Production of composites

Untreated and alkali treated long and short fiber mats were dried in an oven at 80°C for 24 h and placed in a resin bath for about 1 hour. The resin soaked mats were placed in a preheated compression mould and then pressed at 70°C for about 20 min. Three different pressures of 9.4, 10.2, and 12.6 MPa were used to give three different fiber loadings of 40, 50, and 65 wt % respectively. To assess the fiber orientation in the mats, fiber distribution and porosity of composites, samples were

TABLE I
Cellulose, Lignin, and Ash Content of the Untreated and Alkali Treated Hemp Fibers

Sample	Cellulose (%)	Lignin (%)	Ash (%)
Untreated	63.3	4.5	2.6
Alkali Treated	96.7	0.3	0.2

sectioned through their thickness to enable examination of their cross-sections under an optical microscope (Olympus BX 60).

Composite mechanical testing

Composite mats were cut into tensile, flexural, impact and fracture toughness test specimens using a scroll saw according to the specified standard test methods for each of the tests as described below. The samples were then placed in a conditioning chamber at 23°C ± 3°C and 50% ± 5% relative humidity for 40 h.

Tensile testing

Tensile testing was carried out using an Instron-4204 universal testing machine in accordance with ASTM D 638-03 Standard Test Method for Tensile Properties of Plastics with a 5 kN load cell at a rate of 1 mm/min. An Instron 2630-112 extensometer was used to measure strain. Five to six replicates were used.

Flexural testing

Flexural (three point bend) testing was carried out in accordance with the ASTM D 790-03 Standard Test Methods for Flexural Properties of Unreinforced and Reinforced Plastics and Electrical Insulating Materials using a Lloyd LR 100 K universal testing machine fitted with a 5 kN load cell.

Impact testing

Charpy impact testing was carried out in accordance with the International Standard Organization (ISO) 179 Standard Test Method. Dimensions of the samples were 80 mm × 8 mm × 4 mm with a single notch of 0.25 mm (type A). An advanced universal pendulum impact tester POLYTEST with an impact velocity of 2.9 m/s and a hammer weight of 0.475 kg at 21°C was used.

Fracture toughness (K_{Ic}) testing

Single-edge-notch bending (SENB) specimens were obtained in accordance with ASTM D 5045-99 Standard Test Methods for Plane-Strain Fracture Toughness and Strain Energy Release Rate of Plastic Materials. The specimens were tested using a Lloyd LR 100 K tensile testing machine fitted with a 5 kN load cell operating at a rate of 10 mm/min.

RESULTS AND DISCUSSIONS

Lignin and cellulose analysis

It can be seen from Table I that alkali treatment removed about 93% of lignin from hemp fiber. Although specific analysis was not conducted, the resulting high level of cellulose suggests that a large amount of hemicellulose has also been removed.

Scanning electron microscopy (SEM)

Figure 2(a,b) show scanning electron micrographs of untreated and alkali treated fibers. Noncellulosic removal was evidenced by the disappearance of a shiny surface layer and web type features that were present for the untreated fiber resulting in a cleaner surface topography for the alkali treated fiber which could expose rougher and more cohesive surfaces as supported by reference to the literature[26] and would be expected to aid mechanical interlocking in composites.

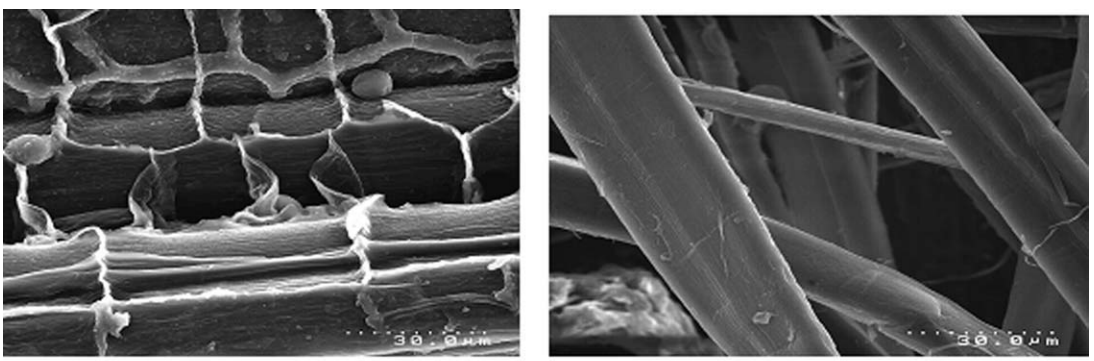

Figure 2 Scanning electron micrographs of (a) untreated and (b) alkali treated fibers.

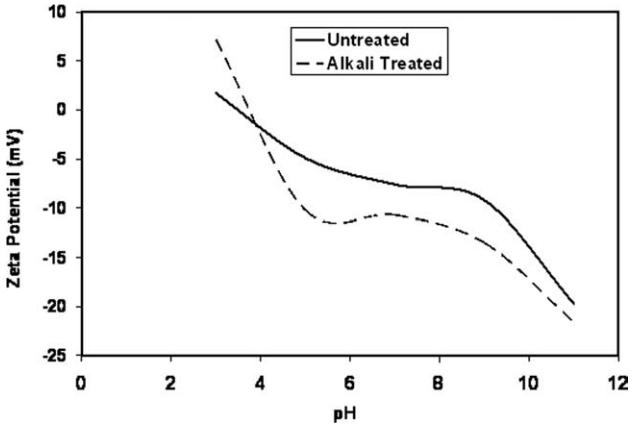

Figure 3 pH dependence of zeta potential of untreated and alkali treated fibers.

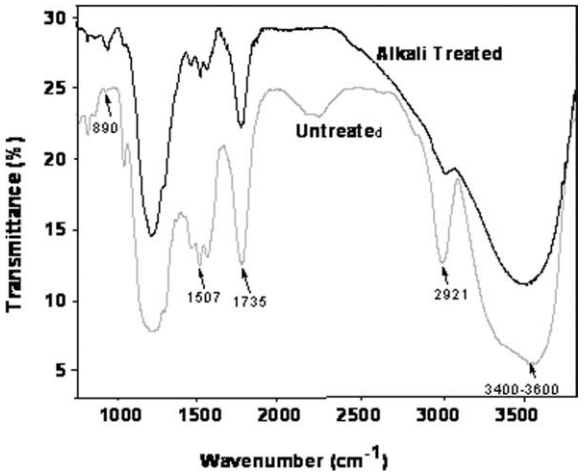

Figure 4 FTIR spectra of untreated and alkali treated fibers.

Zeta potential

Figure 3 shows the pH dependence of zeta potential values of untreated and alkali treated fibers. It is evident from this figure that alkali treatment generally reduces the zeta potential. A considerably lower $\zeta_{plateau}$ value (−11.5 mV) was observed for the alkali treated fibers. This could be caused by the increase in the accessibility of the dissociable functional groups in the fiber surface due to an increased exposure of hydroxyl and carboxyl groups upon removal of the noncellulosic materials that would have initially covered them; hydroxyl and carboxyl groups are known to be responsible for the negative surface charge in cellulosic fibers.[27,28]

The slight increase in the iso-electric point (IEP) for alkali treated fibers highlights the reduction of the acidity of the fiber surface and an enlargement of the double layer giving further evidence for increased —OH group exposure.[29] The enlargement of the double layer would also decrease the zeta potential of the solution as seen.

FTIR spectroscopy

Figure 4 show the FTIR spectra of untreated and alkali treated hemp fibers. For the untreated fiber, peaks in the region of 3400–3600 $cm^{-1,}$ commonly related to stretching vibrations of —OH groups, were found to broaden for treated fibers, supporting the possibility of increased availability of hydroxyl groups. Removal of hemicellulose for alkali treated fibers is suggested by the associated reduction in size of sharp peak at 1735 cm^{-1} present for untreated fibers which is likely to be due to the C=O stretching vibration of carboxylic acid and ester groups present in hemicellulose.[30] Further evidence of hemicelluloses removal is provided by the reduction of peak intensity and peak shift from 2921 cm^{-1} to 2929 cm^{-1} representative of the C—H stretching vibration in hemicellulose.[30] Reduction in the peak intensities between 1448 and 1534 $cm^{-1,}$ especially for the one at 1507 cm^{-1} associated with the bending of C—H bond in aromatic rings present mostly in lignin compounds, suggests the removal of a significant amount of lignin by alkali treatment.[30] The peak at 890 cm^{-1} for untreated fiber, characteristic of the β-glycoside linkage between cellulose monosaccharides, was found to shift to 895 cm^{-1} with an increase in intensity for alkali treated fibers. This may be due to the rotation of the glucose residues around the β-glycosidic bonds which indicates chemical modification of the alkali treated fibers as reported by other authors.[31]

Wide angle X-ray diffraction (WAXRD)

As can be seen in Figure 5, five peaks could be identified for untreated and alkali treated fibers at 2θ-angles of 15, 16.5, 22.5, 34.5, and 46.5° corresponding to $(\bar{1}\ 0\ 1)$, $(\bar{1}\ 1\ 1)$, $(0\ 0\ 2)$, $(\bar{2}\ 3\ 1)$ and $(\bar{4}\ 1\ 2)$

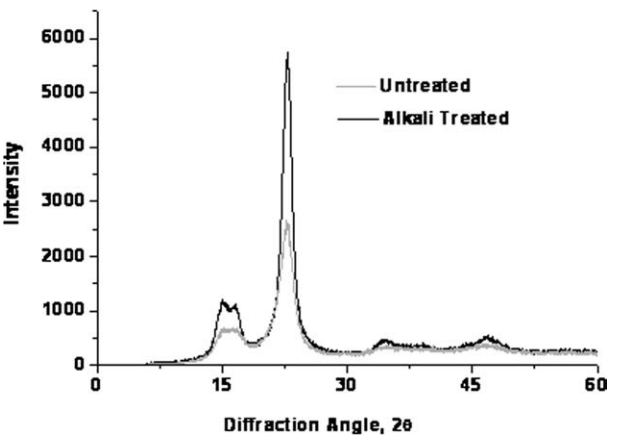

Figure 5 Wide angle X-ray diffractograms of untreated and alkali treated fibers.

TABLE II
The Crystallographic Planes at Various Intensities (XRD counts) and 2θ-angles, and the Crystallinity Indices of Untreated and Alkali Treated Fibers

Sample	2θ-angle (°)	Intensity of WAXRD	h k l	CrI (%)
Untreated	15	571	$\bar{1}$ 0 1	83.8
	16.5	566	$\bar{1}$ 1 1	
	18.5	370	Amorphous	
	22.5	2298	0 0 2	
	34.5	296	$\bar{2}$ 3 1	
	46.5	356	$\bar{4}$ 1 2	
Alkali treated	15	1146	$\bar{1}$ 0 1	91.9
	16.5	1061	$\bar{1}$ 1 1	
	18.5	390	Amorphous	
	22.5	4842	0 0 2	
	34.5	450	$\bar{2}$ 3 1	
	46.5	506	$\bar{4}$ 1 2	

crystallographic planes of cellulose, respectively.[32] It can be observed that the major crystalline peak for both X-ray diffractograms occurred at around $2\theta = 22.5°$, and the intensity of this crystallographic plane (0 0 2) was increased significantly as a result of the alkali fiber treatments.

The crystallinity index (CrI) of untreated and alkali treated hemp fiber samples was calculated using Equation 1 and the results are summarized in Table II. It is worth mentioning that the crystallinity index is generally used for a basis of comparison rather than to define absolute crystallinity.[33] Crystallinity index was found to increase for the alkali treated fibers (Table II) which can be explained by removal of noncellulosic materials enabling better packing of cellulose chains.[34] It can be seen from Figure 4 that the peaks at 15 and 16.5° are merged, appearing more like one broad peak, in the case of untreated fibers and they are separated and more pronounced in the case of alkali treated fibers, again suggesting increased crystalline cellulose for alkali treated fiber; these two peaks have been shown to be separated and pronounced when the fiber contains high amount of crystalline cellulose and merge and appear as one broad peak when the fiber contains large amounts of amorphous material as reported elsewhere.[31]

Thermal analysis

The DTA and TGA thermograms for untreated and alkali treated fibers are shown in Figures 6 and 7 respectively. The DTA thermograms (Fig. 6) for untreated and alkali treated fibers show an endotherm around 60°C due to the evolution of adsorbed moisture. At higher temperatures there are three exotherms. The first exotherm has a peak temperature of about 323°C for untreated fiber and about 360°C for alkali treated fibers and is likely to be caused by thermal depolymerisation of hemicelluloses and pectin.[35] The second exotherm has a peak temperature of 439°C for untreated fiber and around 447°C for alkali treated fibers and is expected to be due to cellulose decomposition.[35] The third exotherm has a peak temperature of 464°C for untreated fiber and around 479°C for alkali treated fibers and is expected to be due to the oxidation of volatile and charred products.[33] The onset, peak and final temperatures of the endotherm and both exotherms described for the alkali treated and untreated fibers are shown in Table III. The increase in the first and second exothermic temperatures for alkali treated fibers indicates their greater thermal stability which could be due to an increase in crystalline cellulose due to better packing of cellulose chains upon alkali treatment as discussed previously. The temperature at which percentage weight losses have occurred (Fig. 7) can be seen to be consistently higher for alkali treated fibers compare to untreated fibers up

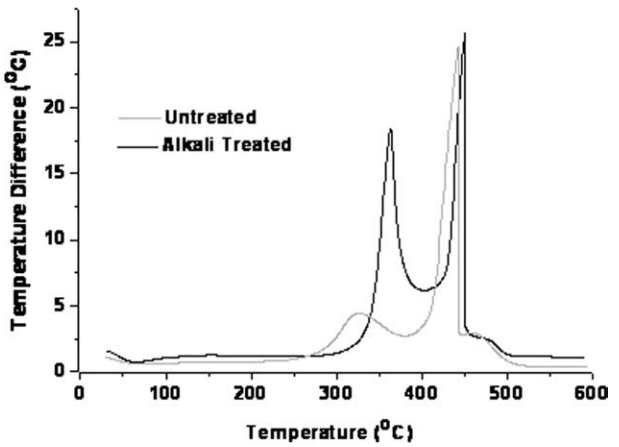

Figure 6 DTA thermograms for untreated and alkali treated fibers in static air flow.

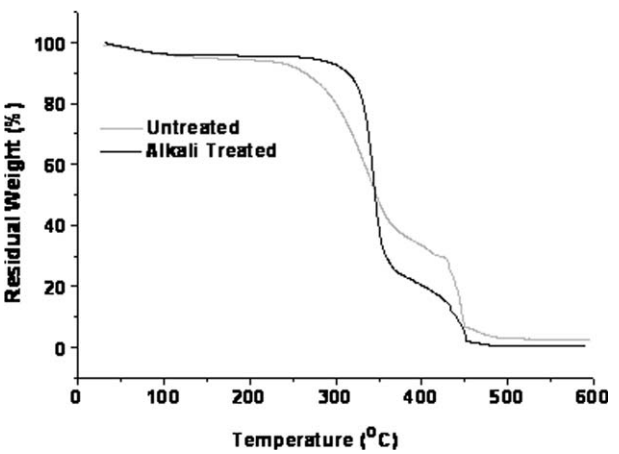

Figure 7 TGA thermograms for untreated and alkali treated fibers in static air flow.

TABLE III
DTA Thermograms, Activation Energy and Frequency Factor for the First and Second Stages of Exothermic Thermal Degradation for Untreated and Alkali Treated Fibers

Sample	Temperature (°C)			Degradation stage	Nature of Peak	E_a (kJ mol^{-1})	Z (s^{-1})
	Onset	Peak	Final				
Untreated	28	57	100	Moisture Evolution	Endo	–	–
	240	323	373	First	Exo	56.1	8.29×10^1
	411	439	441	Second	Exo	50.0	2.10×10^1
	445	464	511	Third	Exo	–	–
Alkali Treated	33	60	121	Moisture Evolution	Endo	–	–
	285	360	398	First	Exo	123.2	6.72×10^7
	413	447	450	Second	Exo	80.7	4.95×10^3
	455	479	511	Third	Exo	–	–

to about 350°C and after that the converse is true, which may be due to stable lignocellulosic complex formed at higher temperature in the more lignin rich untreated fibers and shielding the fiber from weight loss above 350°C.[36]

For various stages of thermal degradation of fibers, the following equation of Broido[37] was used to determine the kinetic parameters E_a and Z (a constant called the frequency factor indicating the number of collisions required for reactions to occur):

$$\ln\left(\ln\frac{1}{y}\right) = -\frac{E_a}{RT} + \ln\left(\frac{RZ}{E_a\beta}T_m^2\right) \quad (2)$$

where y is the fraction of nonvolatilized material yet to decompose, T_m is the peak temperature, β is the heating rate, Z is the frequency factor, E_a is the activation energy, and R is the universal gas constant. Plots of ln[ln(1/y)] versus $1/T$ (Broido plots) for first and second stages of exothermic thermal degradation were obtained for which an example is shown in Figure 8. Approximately linear relationships were found in each instance and the activation energy and frequency factor were calculated from the slopes and intercepts of these plots, respectively, and are given in Table III. Activation energies (E_a) for the first and second exothermic peak for the untreated and alkali treated fibers show that the alkali treated fibers have greater values of activation energies and frequency factors within the range of their respective first and second exothermic peaks. These greater values support increased thermal stability likely to be due to an increase in crystalline cellulose due to better packing of cellulose chains upon alkali treatment of fibers as discussed previously. Ray et al. reported that the thermal stability of the fiber increased in proportion with the increase in crystallinity in cellulose fibers.[19]

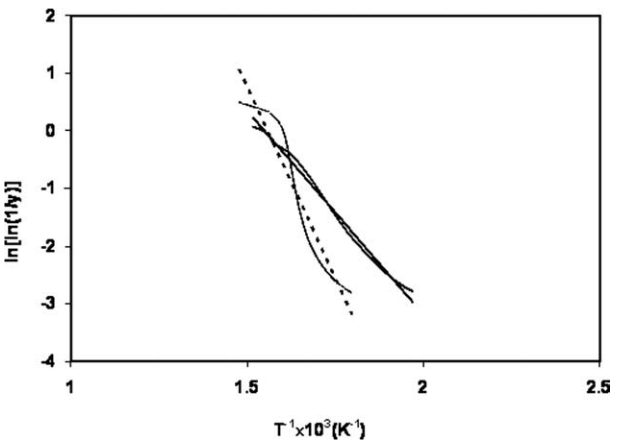

Figure 8 Broido plots for the first stage of exothermic decomposition of untreated (—) and alkali treated (----) fibers.

Single fiber tensile testing

It can be seen from Table IV that alkali treatment reduced average fiber diameter, tensile strength and Young's modulus. Diameter reduction is not surprising considering the expected removal of noncellulosic surface components. Reduced fiber TS and YM could be due to the high percentage of lignin removal or possibly as a result of degradation of cellulose chains.[38]

Composite mechanical properties

Tensile properties

Figure 9 shows the tensile properties of 40 wt % RUS (random untreated short) and RAS (random alkali treated short) fiber/epoxy composites as well as 40, 50, and 65 wt % AUS (aligned untreated short)

TABLE IV
Single Fiber Tensile Test Results of Untreated and Alkali Treated Fibers

Sample	Diameter (μm)	σ (MPa)	E (GPa)
Untreated	32.6 ± 4.9	526 ± 155	34.2 ± 11.3
Alkali Treated	25.9 ± 7.3	463 ± 84	32.8 ± 9.1

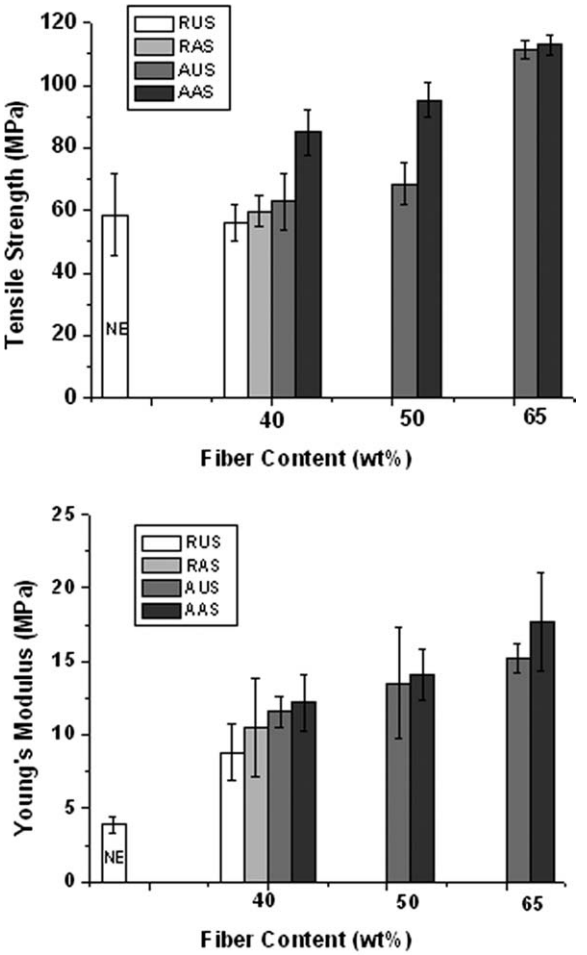

Figure 9 Tensile strength and Young's modulus of 40 wt % RUS and RAS composites and 40, 50, and 65 wt % AUS and AAS composites compared to NE. Each error bar corresponds to one standard deviation.

and AAS (aligned alkali treated short) fiber/epoxy composites compared to neat epoxy (NE). Little increase of TS was seen for untreated and alkali treated randomly oriented fibers compared to NE. Tensile properties of the aligned short fiber/epoxy composites increased as expected compared to the randomly oriented short fiber/epoxy composites indicating that a reasonable extent of alignment of the short fibers had been achieved by dynamic sheet forming. Alkali treated short fiber/epoxy composites had higher TS and YM compared to those for untreated short fiber/epoxy composites (RAS compared to RUS and AAS compared to AUS), which is likely to be due to removal of noncellulosic fiber components and increased surface roughness and the associated increase in —OH groups on the fiber surface which would be compatible with epoxy resin leading to better bonding of alkali treated fibers with epoxy resin. Epoxy resin has active groups known as epoxide or —OH groups to produce a network structure with the active hydrogen atoms of an amine curing agent[3] which can react well with the free —OH groups of the cellulose present in hemp fibers to form very strong covalent bonds in addition to the hydrogen bonds. Increase surface roughness would also increase mechanical interlocking with epoxy resin. An increase in TS and YM was obtained with increased fiber content as observed by other researchers[39,40] demonstrating effective reinforcement by the fibers of the composites. However, fiber treatment was not seen to give the advantage for 65 wt % fiber composites (AAS compared to AUS) that it had at lower fiber contents. To explain this it can be considered that due to the reduction of fiber diameter as described earlier, it would be expected that individual fibers weighed less[9] and therefore, for the same fiber content (wt %) in composites, the number of fibers may be higher for the alkali treated fibers than for untreated fibers. The increase in the number of fibers at higher fiber loadings would increase fiber-fiber contact in the AAS composites such that stress concentration and inefficient stress

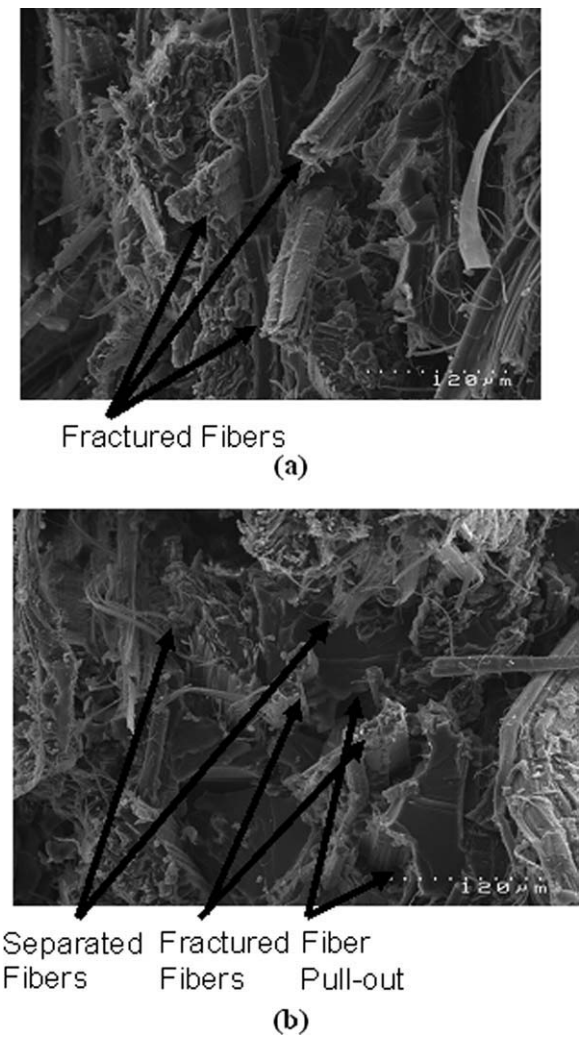

Figure 10 SEM micrographs of fracture surfaces of 65 wt % (a) AUS and (b) AAS composites.

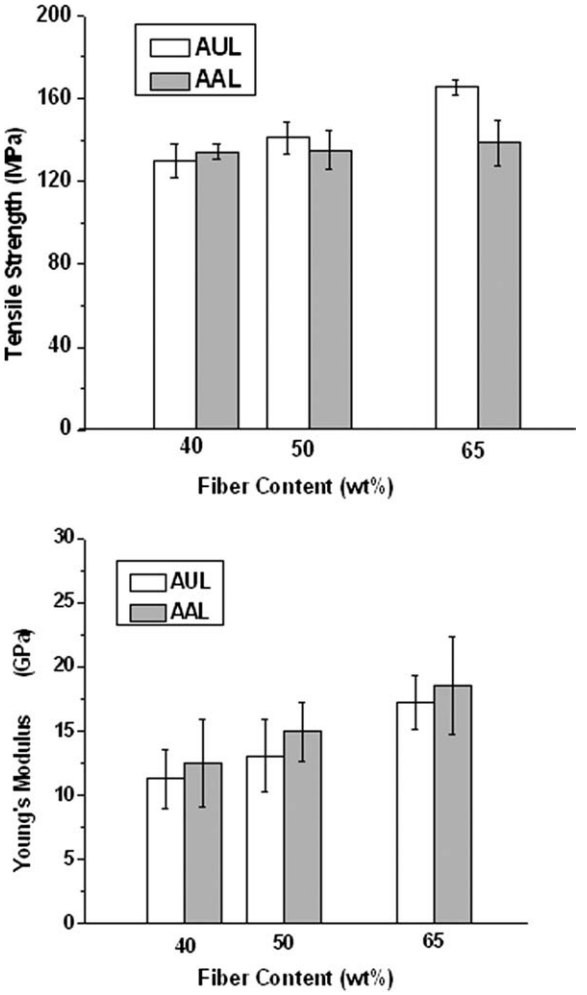

Figure 11 Tensile strength and Young's modulus of 40, 50, and 65 wt % AUL and AAL composites. Error bars each correspond to one standard deviation.

transfer into fibers could occur and limit the mechanical properties.[41,42] This phenomenon of fiber-fiber contact would not be expected to occur at lower fiber contents of alkali treated fiber/epoxy composites as at lower fiber content there should have sufficient resin to wet the fibers.

Figure 10(a,b) show SEM micrographs of fracture surfaces for 65 wt % AUS and AAS composites, respectively. It can be seen that fiber fracture is dominant with untreated and treated fibers, although more pull-out for AAS composites supporting that increased fiber–fiber contact could be initiating more fiber debonding than for AUS composites and limiting mechanical properties.

Figure 11 shows the tensile properties of aligned untreated long (AUL) and aligned alkali treated long (AAL) fiber/epoxy composites at three different fiber contents of 40, 50, and 65 wt %. The TS for long fiber/epoxy composites were found to be 106, 104 and 49% higher for 40, 50 and 65 wt % untreated fibers respectively and 58, 42, and 23% higher for 40, 50, and 65 wt % alkali treated fibers respectively, compared to those for short fiber/epoxy composites. On the other hand, only a slight increase in YM was seen for long fiber/epoxy composites when compared to short fiber/epoxy composites. Similar to short fiber/epoxy composites, an increase in TS and YM for both AUL and AAL composites can be seen with the increased fiber content. At 40 wt % fiber, alkali treatment (AAL compared to AUL) increased TS and YM by 4% and 11% respectively. However, at fiber contents of 50 and 65 wt %, TS was found to decrease for AAL composites compared to AUL composites although YM was still found to increase. Figure 12(a,b) show the SEM micrographs of fracture surfaces of 65 wt % AUL and AAL composites, respectively. Composite fracture with longer separated fibers and holes indicative of more pull-out for AAL composites [Fig. 12(b)] compared to AUL composites [Fig. 12(a)] supports increased fiber-fiber contact for AAL composites has encouraged fiber debonding and reduced TS as seen for short

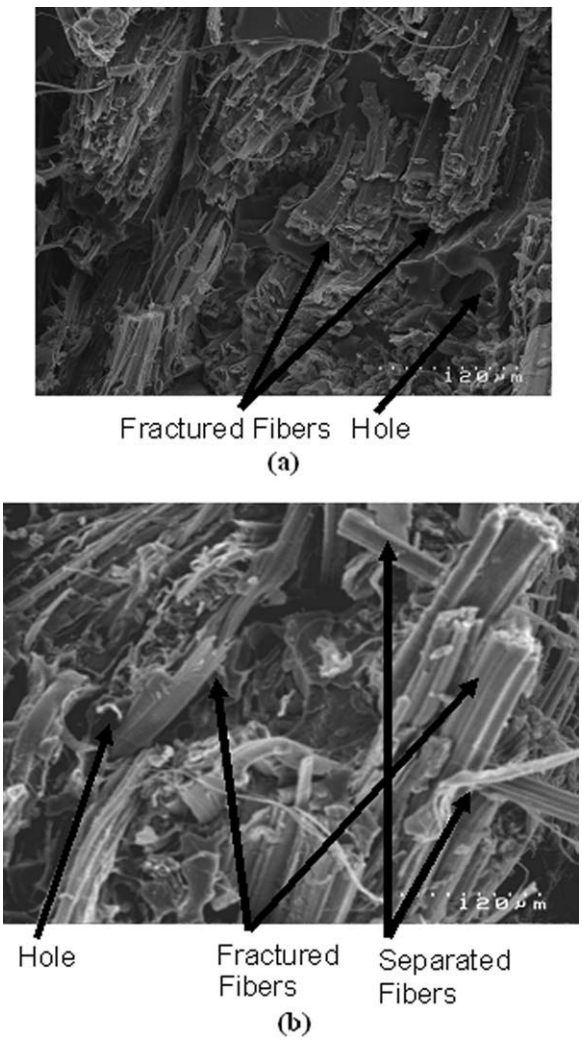

Figure 12 SEM micrographs of fracture surfaces of 65 wt % (a) AUL and (b) AAL composites.

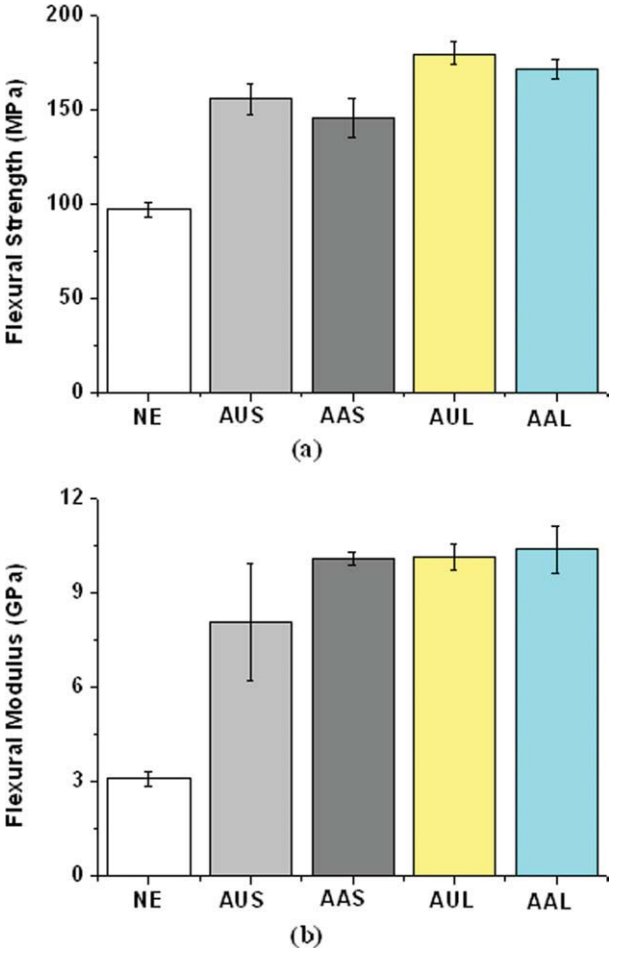

Figure 13 (a) Flexural strength and (b) flexural modulus of 65 wt % AUS, AAS, AUL and AAL composites compared to NE. Each error bar corresponds to one standard deviation. [Color figure can be viewed in the online issue, which is available at wileyonlinelibrary.com.]

fiber/epoxy composites. The reduction in TS in this case suggests that stress concentration is more effective at higher fiber content. The increase in YM can be explained by increased interfacial bonding which would be effective at the early stages of loading before debonding caused by stress concentration at higher loads.

Flexural properties

Figure 13(a,b) show the flexural strength and flexural modulus of composites produced with 65 wt % fiber compared to those for NE. Long fiber composites had the best properties such that flexural strength and flexural modulus were found to be improved compared to NE by up to 85% (AUL) and 235% (AAL) respectively. Treated fiber composites having lower flexural strength but higher flexural modulus suggests that, as for tensile properties, improved interfacial bonding improved modulus,

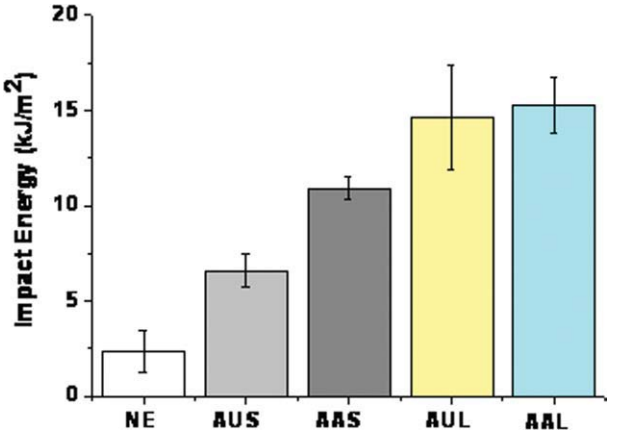

Figure 14 IE of 65 wt % AUS, AAS, AUL, and AAL composites compared to NE. Each error bar corresponds to one standard deviation. [Color figure can be viewed in the online issue, which is available at wileyonlinelibrary.com.]

but stress concentrations due to fiber–fiber contact limited strength.

Impact energy (IE)

Figure 14 shows the IE of composites produced with 65 wt % fiber compared to that for NE. From the results it can be seen that the IE for AUS and AAS composites was between 3 and 6 times the IE of NE which is likely to be due to increased dissipation of energy by fiber pull-out. Improvement in IE has also been observed by Acha et al. who obtained an increase of more than three times of the IE of untreated jute fiber composites compared to the brittle unsaturated polyester matrix.[43] Higher IE was seen in the current work for treated fiber composites compared to untreated fiber composites (Fig. 14)

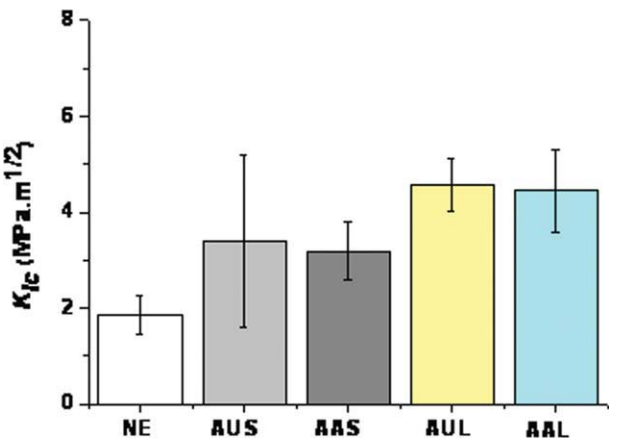

Figure 15 K_{Ic} of 65 wt % AUS, AAS, AUL, and AAL composites compared to NE. Each error bar corresponds to one standard deviation. [Color figure can be viewed in the online issue, which is available at wileyonlinelibrary.com.]

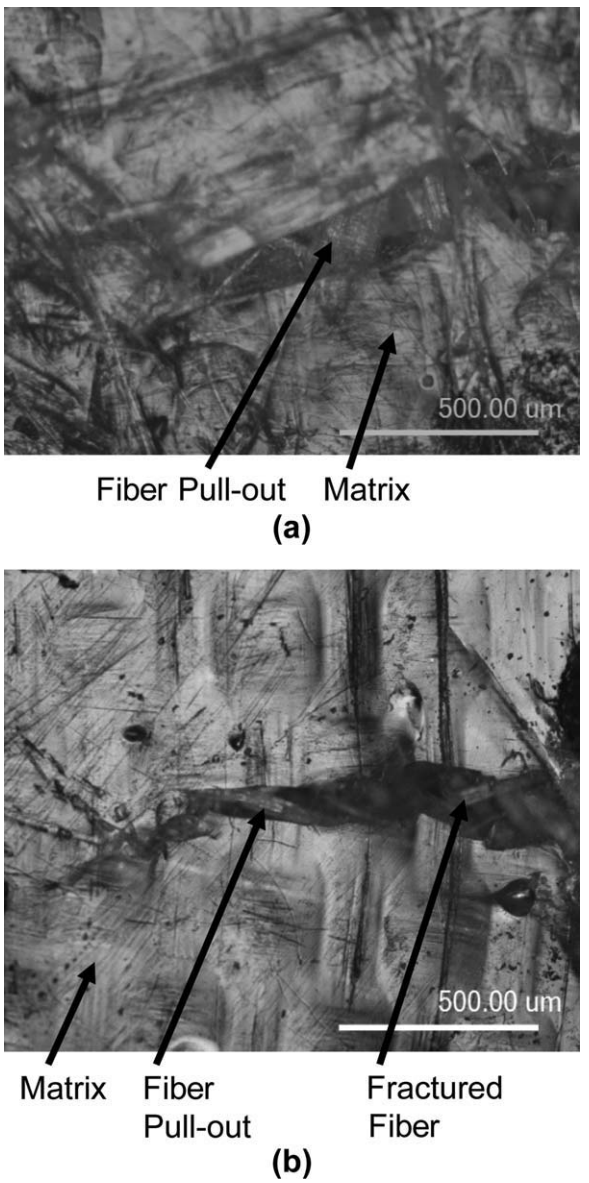

Figure 16 Optical micrographs showing major crack of fracture toughness specimens of (a) AUL and (b) AAL composites.

which might be due to more fiber pull-out and delamination for treated fiber composites due to increased fiber/fiber contact.

IE for long fiber/epoxy composites (Fig. 14) was over six times higher than that for NE. Similar to short fiber/epoxy composites, the IE of AAL composites was found to be higher than that for AUL composites.

Fracture toughness (K_{Ic})

Figure 15 shows the K_{Ic} of composites produced with 65 wt % fiber compared to that for NE. K_{Ic} was higher for the composites than for NE[44] as reported by other researchers.[44] A slight decrease in K_{Ic} was seen here for treated fiber composites compared to that for untreated fiber composites possibly due to easier debonding of fiber from the epoxy resin matrix as a consequence of increased fiber–fiber contacts in treated composites as previously discussed. Support for this being due to the ease of pull out as a result of increased fiber contact was seen in the form of more pull out and less fiber failure for AAL composites [Figs. 16(a,b)].

CONCLUSIONS

Alkali treatment was shown to remove noncellulosic components from hemp fiber resulting in better separated fibers with cleaner surface topography, increased cellulose crystallinity and better thermal stability. The tensile strength was found to be reduced which is believed to be due to a degree of degradation of cellulose chains and too much lignin removal. Decrease in zeta potential indicated increased exposure of —OH groups.

Tensile properties of short fiber/epoxy composites produced by aligning the fibers along the tensile testing axis were found to increase compared to randomly oriented short fiber/epoxy composites. Alkali treatment also improved the TS and YM of short fiber/epoxy composites.

Long fiber/epoxy composites were found to show consistently higher mechanical properties than those for short fiber/epoxy composites. At 40 wt % fiber, treated fiber provided the most effective reinforcement, however, at fiber contents of 50 and 65 wt %, TS was found to decrease as a result of fiber treatment, although YM was still found to increase, which is believed to be due to increased fiber–fiber contact in the treated fiber composites such that stress concentration leads to a reduction in TS despite increased interfacial strength. Flexural strength and K_{Ic} were found to increase and IE was found to decrease for aligned untreated fiber/epoxy composites which is likely to be due to the increased stress concentration by increased fiber-fiber contact in aligned alkali treated fiber/epoxy composites.

References

1. Robson, D.; Hague, J.; Newman, G.; Jeronomidis, G.; Ansell, M. In Survey of Natural Materials for Use in Structural Composites as Reinforcement and Matrices; Woodland Publishing Ltd: Abingdon, 1996.
2. Saheb, D. N.; Jog, J. P. Adv Polym Technol 1999, 18, 351.
3. Matthews, F. L.; Rawlings, R. D. Composite Materials: Engineering and Science; Chapman and Hall: London, New York, 1994.
4. Pickering, K. L.; Priest, M.; Watts, T.; Beckermann, G.; Alam, S. N. J Adv Mater 2005, 37, 15.
5. Thomsen, A. B.; Bohn, V.; Nielsen, K.; Pallesen, B.; Jorgensen, M. S. Bioresour Hemp 2000, 13-16, 1. Available at www.nova-institut.de.

6. Rowell, R. M. In Proceedings of the International Conference on Science and Technology of Composite Materials (COMAT 2001); Mar del Plata; Argentina, 2001.
7. Chang, H. M.; Cowling, E. B.; Brown, W.; Adler, E.; Miksche, G. Holzforschung 1975, 29, 153.
8. Gassan, J.; Bledzki, A. K. J Appl Polym Sci 1999, 71, 623.
9. Gassan, J.; Bledzki, A. K. Compos Sci Technol 1999, 59, 1303.
10. Prasad, S. V.; Pavithran, C.; Rohatgi, P. K. J Material Sci 1983, 18, 1443.
11. Islam, M. S.; Pickering, K. L. Adv Mater Res 2007, 29-30, 319.
12. Valadez-Gonzalez, A.; Cervantes-Uc, J. M.; Olayo, R.; Herrera-Franco, P. J. Composites B 1999, 30, 309.
13. Herrera-Franco, P. J.; Valadez-Gonzalez, A. Composites B 2005, 36, 597.
14. Bledzki, A. K.; Fink, H. P.; Specht, K. J Appl Polym Sci 2004, 93, 2150.
15. Khalil, H. P. S. A.; Ismail, H.; Ahmad, M. N.; Ariffin, A.; Hassan, K. Polym Int 2001, 50, 395.
16. Bledzki, A. K.; Reihmane, S.; Gassan, J. J Appl Polym Sci 1996, 59, 1329.
17. Mukherjee, R. N.; Pal, S. K.; Sanyal, S. K. J Appl Polym Sci 1983, 28, 3029.
18. Zadorecki, P.; Flodin, P. J. J Appl Polym Sci 1985, 3, 3971.
19. Ray, D.; Sarkar, B. K.; Basak, R. K.; Rana, A. K. J Appl Polym Sci 2004, 94, 123.
20. Varley, R. J.; Hodgkin, J. H.; Hawthorne, D. J.; Simon, G. P.; Mcculloch, D. Polymer 2000, 41, 3425.
21. Wang, H. M.; Postle, R. Text Res J 2003, 73, 664.
22. Goerge, J.; Ivens, J.; Verpoest, I. Die Angew Makromoleculare Chem 1999, 272, 41.
23. Mohanty, A. K.; Khan, M. A.; Hinrichsen, G. Compos Part A: Appl Sci Manufacturing 1999, 3, 143.
24. Goutianos, S.; Peijs, T.; Nystrom, B.; Skrifvars, M. Appl Composite Mater 2006, 13, 199.
25. Segal, L.; Creely, J.; Martin, C. M. Text Res J 1959, 29, 786.
26. Bessadok, A.; Marais, S.; Roudesli, S.; Lixon, C.; Metayer, M. Compos Part A: Appl Sci Manufacturing 2008, 39, 29.
27. Kleinschek, K. S.; Ribitsch, V. Colloids Surf A: Physicochemical Eng Aspects 1998, 140, 127.
28. Clark, J. A. Pulp Technology and Treatment for Paper; Miller Freeman and Publications, Inc.: San Francisco, 1985.
29. Bismarck, A.; Aranberri-Askargorta, I.; Springer, J.; Lampke, T.; Wielage, B.; Stamboulis, A.; Shenderovich, I.; Limbach, H. Polym Compos 2002, 23, 872.
30. Ray, D.; Sarkar, B. K. J Appl Polym Sci 2001, 80, 1013.
31. Tserki, V.; Zafeiropoulos, N. E.; Simon, F.; Panayiotou, C. Composites: Part A 2005, 36, 1110.
32. JCPDS-International Centre for Diffraction Data, 2.4, 2003.
33. Ouajai, S.; Shanks, R. A. Polym Degrad Stab 2005, 89, 327.
34. Mwaikambo, L. Y.; Ansell, M. P. J Appl Polym Sci 2002, 84, 2222.
35. Troedec, M.; Peyratout, C.; Smith, A.; Chotard, T. J Eur Ceram Soc 2009, 29, 1861.
36. Ray, D.; Sarkar, B. K.; Basak, R. K.; Rana, A. K. J Appl Polym Sci 2002, 85, 2594.
37. Broido, A. J Polym Sci 1969, 7, 1762.
38. Beckermann, G. W.; Pickering, K. L.; Foreman, N. J. In Proceedings of the 2nd International Conference on Structure, Processing and Properties of Materials (SPPM 2004); Dhaka, Bangladesh; 2004; 257–265.
39. Hill, C. A. S.; Khalil, H. P. S. A. J Appl Polym Sci 2000, 78, 1685.
40. Sanadi, A. R.; Prasad, S. V.; Rohatgi, P. K. J Mater Sci 1986, 21, 4299.
41. Sreekala, M. S.; Thomas, S.; Neelakantan, N. R. J. Polym Eng 1997, 16, 265.
42. Pal, S. K.; Mukhopadhyay, D.; Sanyal, S. K.; Mukherjea, R. N. J Appl Polym Sci 1988, 35, 973.
43. Acha, B. A.; Marcovich, N. E.; Reboredo, M. M. J Appl Polym Sci 2005, 98, 639.
44. Yan, L. Acta Mechanica Solida Sinica 2004, 17, 95.